Segmental rotor switched reluctance motors with single-tooth windings

B.C. Mecrow, E.A. El-Kharashi, J.W. Finch and A.G. Jack

Abstract: Switched reluctance machines with segmental rotors are investigated, building on previous work which has produced high torque prototypes. The paper presents a machine topology, which permits the use of short pitched windings placed around a single-tooth. This concept maintains the torque capability of a previous design, but uses much less copper volume. The theoretical basis for the machine configuration is developed and then the results for a working prototype machine are shown, illustrating static torque and flux linkage profiles. Results are presented for the machine operating as a drive, indicating the viability of the concept.

List of principal symbols

A	magnetic vector potential
i	phase current
R	phase resistance
t	width of airgap which actively carries magnetic flux in the aligned position
V	phase voltage
λ	rotor pole pitch
ψ	flux-linkage

1 Introduction

In earlier papers the authors have introduced the concept of using a segmental rotor design for switched reluctance motors (SRMs) [1, 2]. Instead of the usual toothed arrangement the rotor is constructed from a series of discrete segments, each of which is magnetically isolated from its neighbour. Torque results as the rotor segments modulate the stator slot permeance, which is minimised when the segments are centred under a stator tooth, and maximised when the segments bridge a slot opening.

Single-phase machines were initially considered [1], and it was shown to be possible to create greater airgap force densities than with conventional toothed rotors once the ratio of effective tooth width to pole pitch exceeded 0.5. The general concept was then applied to three-phase machines, which naturally led to a design in which the coils span a number of slots. A prototype machine was built and measurements indicated that it could deliver over 40% more torque than a conventional SRM within a given frame size. However, the machine had substantially longer end-windings, which reduced the electric loading and made it impractical for applications which combined a short lamination stack length with a large pole pitch.

IEE Proceedings online no. 20030366

doi:10.1049/ip-epa:20030366

Paper first received 17th October 2002 and in revised form 27th January 2003. Originally published online: 12th May 2003

The authors are with the School of Electrical, Electronic and Computer Engineering, University of Newcastle Upon Tyne, Merz Court NE1 7RU, UK

This paper addresses the challenge of producing a three-phase segmental rotor SRM with short, nonoverlapping end-windings [3]. The general concept behind the chosen geometry is developed and analysed, before progressing to the detailed design and construction of a demonstrator machine. Static and running test results are presented, enabling an objective evaluation of the concept.

2 Machine concept

The rotor structure of these machines is similar to that of segmental rotor synchronous reluctance motors developed in the 1960s [4, 5]. However, the stator is somewhat different: the windings are concentrated, there is negligible coupling between phases and the excitation uses pulses of direct current rather than sinusoidal AC current. The concept has more similarities with the earlier work of Xu and Lipo [6–8], who developed a two-phase axially laminated reluctance machine. Although Xu and Lipo regarded their machine as a synchronous reluctance motor, it had concentrated windings and was operated in a switched fashion, similar to the machines presented here. Horst [9] appears to be the only other researcher to combine a segmental rotor construction with a switched reluctance stator; he patented the concept of a two-phase segmental rotor for unidirectional operation.

To develop the new design with nonoverlapping end-windings it is necessary to revisit the basic design concept and establish some design rules. These will be applied to a rectilinear geometry before progressing to a full rotating machine design.

Fig. 1 shows a rectilinear single-phase machine in which each stator coil encloses a single-tooth, along with the magnetic flux distribution in the aligned position. The magnetic flux flows down one tooth, through a rotor segment and returns via the adjacent stator tooth. All the conductors in each slot only couple with flux driven by their own magneto-motive force, with very little mutual coupling between one slot and another. Torque production can therefore be envisaged on a per slot basis in which the slot MMF drives flux round the slot and the slot permeance is modulated by the rotor segments. The ratio of maximum to minimum slot permeance is a function of machine size and geometry, and has been measured to be approximately five for an unsaturated machine of 150 mm diameter. Any one magnetic flux path is excited by the net MMF within a slot

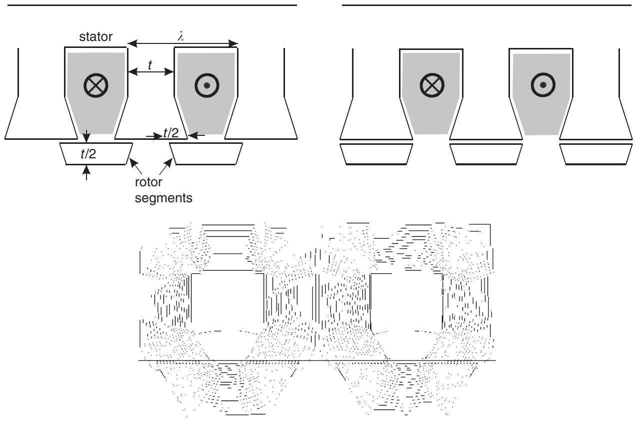

Fig. 1 *Rectilinear representation of a single-phase segmental rotor SRM, showing aligned position, unaligned position and a magnetic flux plot in aligned position*

and therefore, if mutual coupling between phases is to be avoided, each slot should only contain the conductors of a single-phase. In single-phase machines this condition is met by default, but in multiphase conventional SRMs each slot generally shares the conductors of two phases, so the standard winding method of placing coils around a single-tooth and winding every tooth is no longer valid. In [1] the solution adopted for a multiphase design was to employ a concentrated winding in which each coil spanned as many stator teeth as there were phases.

The above design has produced excellent results in a prototype machine with 12 stator teeth and eight rotor segments (henceforth referred to as a 12-8 machine) [1]. This design, in which the stator teeth span one complete magnetic pole, has fully pitched windings. It will be subsequently referred to as the 'multitooth winding' design, reflecting the coil span. In comparison with conventional SRMs the flux-linkage per phase has been effectively doubled, so that the torque as a function of electric loading is also doubled. This is because the effective tooth width to rotor pole pitch, t/λ, can be increased to more than 0.7 without the unaligned permeance becoming prohibitively large. The increase in magnetic utilisation of the machine is evident as the flux of a single-phase is now carried by two-thirds of the stator teeth rather than the one-third used in a conventional three-phase SRM. However, because the coils must span three stator teeth, the end-winding is much longer than in a conventional 'single-tooth winding' SRM. This additional end-winding loss forced a 20% reduction in electric loading in the prototype machine at thermal limit. The doubling of flux-linkage, coupled with a reduction in electric loading, gave a 40% net increase in the measured torque per unit volume at thermal limit, but only a modest rise in the torque per unit winding mass. The prototype has a stack length equal to the outside diameter of the stator, but if the ratio of stack length to outside diameter were to be reduced the influence of the end-windings would become larger. Consequently, for machines of short stack length the concept will no longer be attractive.

To develop a three-phase design which is suitable for short stack length machines it is essential that the winding spans a single-tooth to keep the end-windings short, whilst maintaining the condition that only the conductors of a single-phase occupy any one slot. To see how this is achieved, Fig. 2 shows the multitooth winding design in rectilinear form, illustrating the conductors of a single-phase. It can be seen that each coil actually spans two rotor

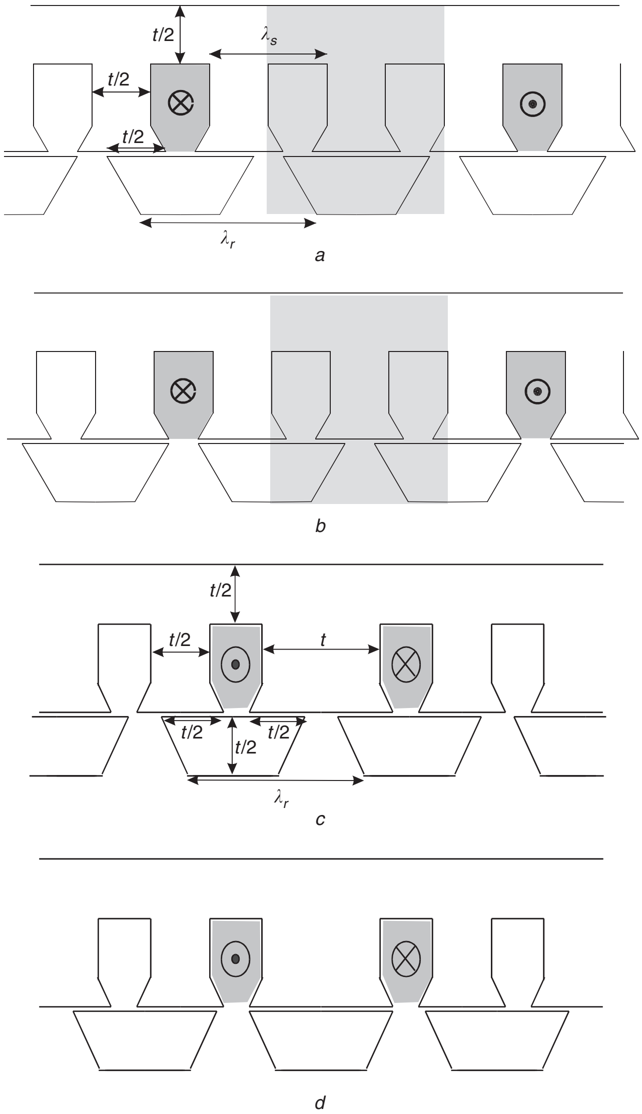

Fig. 2 *Rectilinear representation of three-phase segmental SRMs*
a Multitooth winding machine in aligned position
b Multitooth winding machine in unaligned position
c Single-tooth winding machine in aligned position
d Single-tooth winding machine in unaligned position

segments. If the region shown shaded were removed then the coil would span a single rotor segment and would have a shorter end-winding, wrapped round a single-tooth. In the resulting 'single-toothed winding' arrangement, which is also illustrated in Fig. 2, the stator teeth form two separate groups: double-width teeth, which are enclosed by a winding, and standard-width teeth which are unwound. The unwound teeth still have a function, as they act as return paths for the magnetic flux. Excitation of a single-phase now excites two adjacent slots and the phase permeance is the sum of the two slot permeances. The tooth pitch of the wound stator teeth must be equal to the rotor pole pitch, so that the permeance variation of these two slots with respect to rotor position is in phase.

Fig. 3 shows the flux distribution in both the multitooth and the single-tooth winding designs, with a single-phase excited. Both the aligned position and the unaligned position are shown. In both cases the rotor pole pitch is maintained at 20 mm, the airgap length is 0.3 mm and the effective ratio of t/λ is 0.67. (In conventional toothed rotor SRMs the ratio of tooth width t to rotor pole pitch λ is used because it gives a measure of the magnetic utilisation of the machine. In a segmental rotor machine the concept of tooth

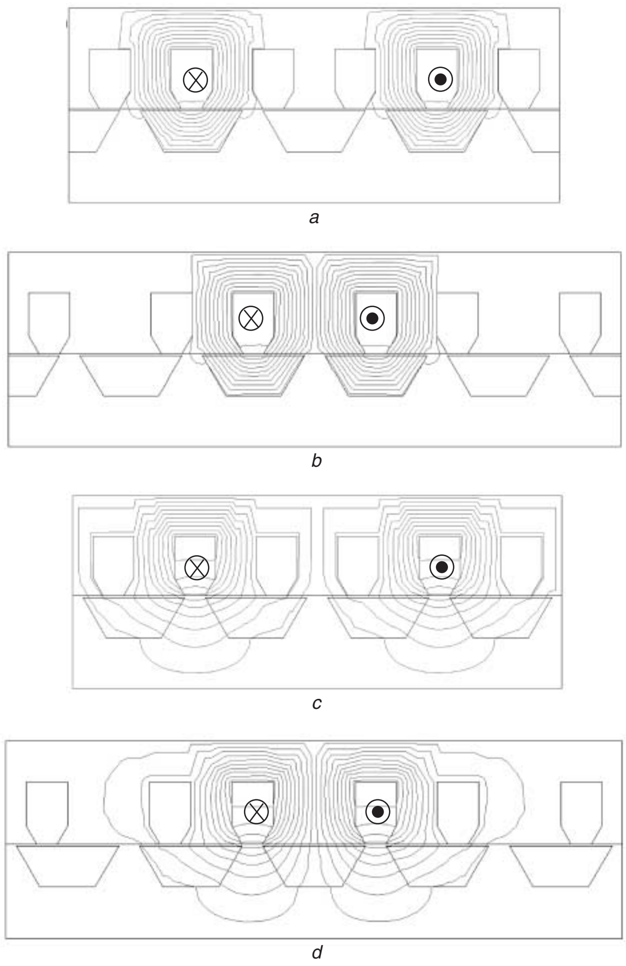

Fig. 3 *Flux plots showing magnetic flux distribution in both three-tooth and single-tooth winding segmental rotor SRMs*
a multitooth design, aligned position
b single-tooth winding design, aligned position
c multitooth design, unaligned position
d single-tooth winding design, unaligned position

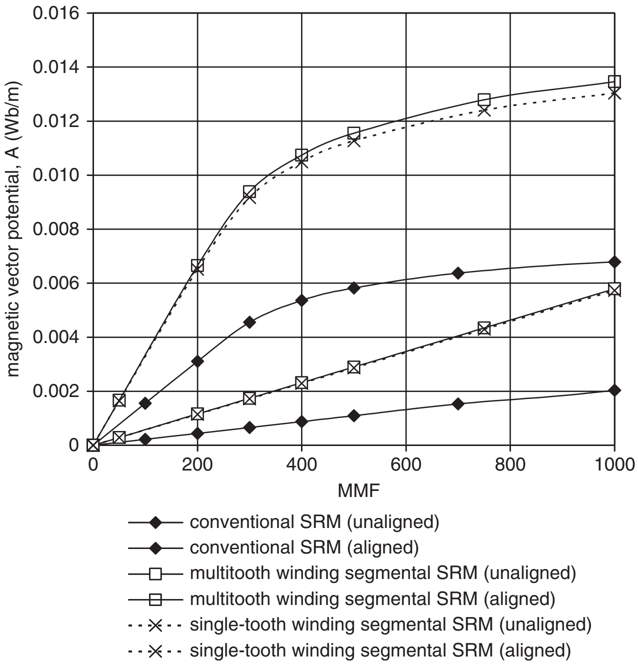

Fig. 4 *Magnetic vector potential of a phase coil as a function of coil MMF for both segmental designs and a conventional SRM*

width is not applicable, since the rotor has no teeth. However, the notation t/λ will continue to be used to denote the wider definition of 'the proportion of the machine airgap over an excited rotor pole which carries airgap flux in the aligned position.')

The two designs have identical slot shapes and cross-sectional areas and identical core back depths. The unwound teeth of the single-tooth winding design are the same width as each of the teeth of the multitooth winding design, whilst the wound teeth are double this width. The flux plots for the two machines are very similar, except for the fact that two stator slots and one stator tooth have been removed in the single-tooth winding design. As these regions carried no flux, their removal does not significantly influence the level of flux-linkage.

Fig. 4 shows two-dimensional finite element predictions of the flux-linkage curves per unit axial length for the two designs and, as might be expected, they are virtually identical. Indeed, in the unaligned position the two permeances are within 1% of each other, whilst in the aligned position the unsaturated permeances are almost identical and the saturated values are within 3%. As the flux-MMF curves are identical, so is the force produced by any one phase. Fig. 4 also shows flux-linkage curves for the equivalent conventional SRM with a toothed rotor, indicating how its flux-linkage amounts to only one-half of the segmental designs.

The reasoning above seems to suggest that the single-tooth winding design has all the advantages of the multitooth winding design, but with shorter end-windings. However, in reality the comparison is more complicated. The three-phase coils of the multitooth winding design occupy a peripheral length of four rotor segments, whilst the three-phase coils of the single-tooth winding design occupy five segments because the wound teeth are increased in width. Consequently, in the single-tooth winding design the force exerted per unit area of airgap is reduced to only 80% of the multitooth winding design when the MMF per phase is fixed. It can now be seen that the single-tooth winding design has much shorter end-windings, thereby permitting an increased phase MMF for a given loss, but utilises the magnetic circuit less well, so that the force density per unit MMF is reduced by 20%.

3 Design rules

For clarity a complete set of design rules for the single-tooth winding design are given below:

1. Only one phase winding is contained in any one slot.
2. All coils span a single slot.
3. Only every other slot is wound in order to satisfy rules 1 and 2.
4. The pitch between two adjacent stator slots carrying the MMF of one phase is equal to the rotor pole pitch, so that the slot permeances of each phase all vary in phase with each other.
5. The width of the gap between rotor segments is equal to that of the stator slot openings. This ensures that neither the rotor nor stator contribute unnecessarily to the unaligned permeance.
6. The width of the body of the wound stator teeth is equal to twice the width of overlap between one rotor segment and the tooth tip in the aligned position. This ensures that the flux density in the body of the tooth is equal to that in the tooth tips.

7. The width of the body of the unwound teeth is equal to one-half that of the wound teeth, as two unwound teeth carry the return flux of one wound tooth.

8. The radial depth of both the stator core back and the rotor segments is equal to the width of the unwound tooth as they only ever carry the flux of one unwound tooth.

4 Three-phase single-tooth winding demonstrator

A three-phase rotating demonstrator has been designed in accordance with the above rules, and then built and tested. A design with one coil per phase requires five rotor segments, but then excitation of a single-phase acts on only one side of the rotor, producing a large unbalanced magnetic pull. For this reason a 12-10 design was adopted, with the stator arrangement shown schematically in Fig. 5. There are now two coils per phase, with the two coils diametrically opposite each other. The machine's overall dimensions were chosen to be identical to those of other SRMs built at the University of Newcastle, resulting in an outside diameter of 150 mm and a lamination axial stack length, also of 150 mm.

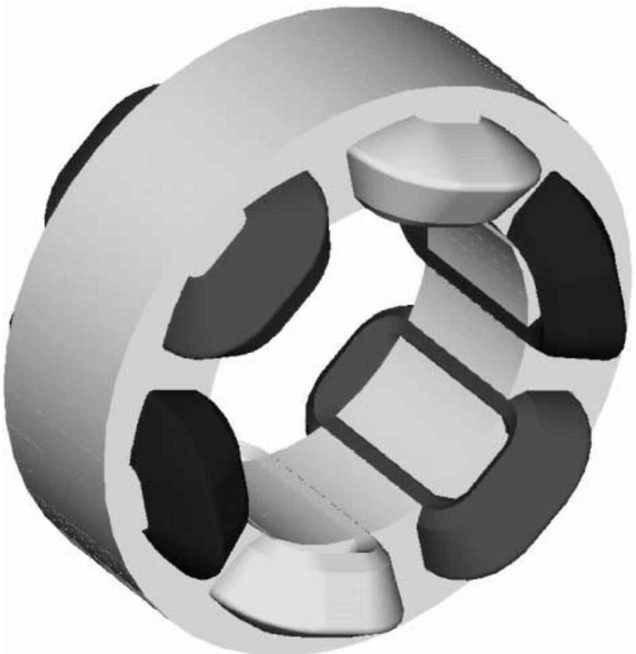

Fig. 5 *General machine arrangement for a 12–10 three-phase SRM with single-tooth windings*

Fig. 6 *Rotor of 12–10 single-tooth SRM, showing individual rotor segments*

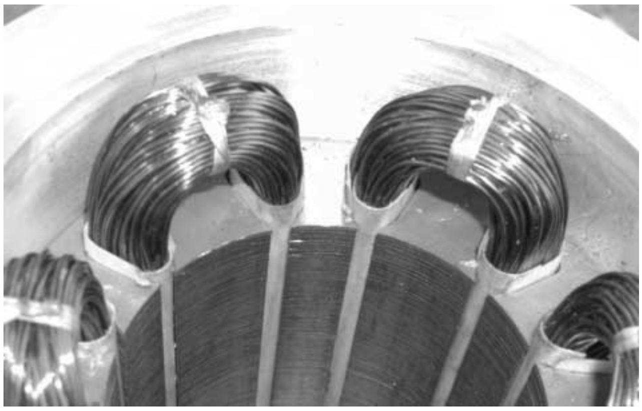

Fig. 7 *Close-up of the stator of 12–10 segmental rotor SRM, showing nonoverlapping windings, placed around every other tooth*

Fig. 6 is a photograph of the segmental rotor, showing the laminated segments mounted onto a nonmagnetic shaft. The method of assembly is identical to that of the 12-8 multitooth winding segmental machine, and readers may refer to [1] for further details. Fig. 7 is a photograph of the single-tooth winding stator, clearly showing the winding arrangement, with each coil wound around a single-tooth, and only every other tooth wound. The laminations are shrunk into a totally enclosed aluminium frame, which is then fan cooled at its surface. Table 1 gives full dimensional details of the prototype, alongside those of the multitooth winding machine and a toothed rotor SRM with fully pitched windings. Extensive test results were available for the two earlier machines, enabling an objective comparison.

Fig. 8 illustrates the magnetic flux distribution within the machine with one phase excited. This phase has two coils, wound around the two horizontal teeth. Two plots are shown, corresponding to the aligned and unaligned positions. The path of the magnetic flux linking each coil is isolated from both that of the other phases and the other coils of the same phase. Unlike a conventional SRM there is no mutual coupling between phases through cross-slot leakage flux, but a small degree of mutual coupling occurs via the stator core back and next wound tooth.

The machine was wound with 1.0 mm-diameter conductors, as in the multitooth winding segmental SRM. The two machines have virtually identical slot areas but, because the effective slot fill factor fell from 0.46 to 0.41 there was a 10% reduction in the number of series turns per phase. The mean end-winding length is reduced from 124 mm to 67 mm, resulting in a reduction of 20% in the mean turn length.

5 Static performance

The prototype machine has been subjected to static torque testing, and the measured torque–position curves are shown in Fig. 9. At high currents the torque variation with position is almost sinusoidal in shape, in a manner consistent with conventional SRMs operating with high magnetic saturation. At low currents the machine is operating in a

Table 1: Dimensions of the prototype machines and a fully pitched winding toothed rotor SRM, used for comparison

	Single tooth winding segmental rotor SRM	Multi tooth winding segmental rotor SRM	Toothed rotor SRM
Number of phases	3	3	3
Number of stator slots	12	12	12
Number of rotor segments/teeth	10	8	8
Outside diameter, mm	150.0	150.0	152.6
Stack axial length (rotor and stator), mm	150.0	150.0	150.00
Rotor outside diameter, mm	90.8	90.8	89.6
Airgap length, mm	0.3	0.3	0.25
Stator tooth width, mm	20.0/10.0	11.93 (parallel sided)	12.05 at tip, with 12 degree taper
Arc of stator tooth tip, deg.	30.25/18.5	22.5	15.0
Stator core back depth, mm	10.00	11.9	10.6
Arc of rotor segments/teeth, deg.	30.25	37.5	16.2
Number of series turns/phase	270	300	204
Coil span	1 widetooth (36 mechanical degrees)	3 slots (90 mechanical degrees)	3 slots (90 mechanical degrees)
Effective wire diameter, mm	1.0	1.0	1.20
Estimated turn length, mm	435	547	591
Slot fill-factor (copper area to overall slot area), %	41	46	42
Resistance per phase @ 20 °C, Ω	2.56	3.58	1.825

magnetically linear mode, and significant torque is produced between the aligned position and a displacement of 12 mechanical degrees, corresponding to one-third of an electrical cycle. Once more this is typical of any SRM, but unlike conventional machines the torque profile is not flat; within the torque producing region it rises with displacement from the aligned position, producing a peak at approximately 12°. This is because the permeance of a phase winding does not change linearly with position. This effect was encountered on the multitooth winding segmental SRM – further discussion of the effect can be found in [2].

Locked rotor tests were used to determine the flux-linkage–current-position characteristics. A DC voltage was applied to one phase and the current monitored. The flux-linkage was then determined using the equation

$$\psi = \int_0^t [V - iR]\, dt \qquad (1)$$

Fig. 10 shows the results of these tests for a series of positions, ranging from the unaligned to aligned position. Fig. 11 compares the measurements with those predicted using two-dimensional finite elements. The measured and predicted curves for the aligned position are within 2% of the peak flux-linkage, but the predicted unaligned flux-linkage is 17% less than the measured value. Predicted values take no account of end-winding leakage inductance, and this will be the major cause of this error. This leakage component is also present in the aligned position, but is reduced in its influence at high excitation currents by saturation of the machine core.

The finite element analysis was also used to predict the static torque performance indirectly from the flux-linkage curves. Comparisons with measured values are shown in Fig. 12 for four different excitation levels. In all cases the agreement between predicted and measured values is good, with the predicted torques having the correct shape of the torque profile but typically overestimating the torque produced by 5%. This is a direct result of underestimating the unaligned permeance, as discussed above.

6 Orientation of magnetisation

There is the freedom to choose the magnetic orientation of each coil, and the effect of this can be understood by initially considering excitation of a single-phase. Each phase is constructed from two coils, positioned at opposite sides of the machine. The magnetic flux plots of Fig. 8 show that there is minimal coupling between the individual phase coils of a phase. Consequently the magnetic characteristics of any one phase are independent of the polarity of the two coils: both may have an MMF directed radially inwards, both outwards, or one in each direction without having a measurable effect on the phase parameters.

Consider now the situation when two phases are simultaneously excited. There are two mechanisms by which the two phases can interact: either due to mutual magnetic coupling or to cross-saturation of their common magnetic flux paths. The mutual inductance between phases has already been shown to be minimal, leaving only the cross-saturation effect. In conventional SRMs the rotor and stator core backs carry the flux of all phases: to prevent cross-saturation when multiple phases are excited it is often necessary for the core back to be deeper than that magnetically required by one phase acting alone. In the segmental machine the situation is somewhat different. Each portion of stator core back and each wound tooth carries only the flux of one phase and therefore can be sized accordingly. Only the unwound teeth, forming the flux return path, contain the flux of two phases. If the phase coil MMFs all act inwardly then the return fluxes of two excited phases are both outward and the flux in the unwound tooth will be the sum of the two phase fluxes. The teeth have been dimensioned to only take the flux of a single-phase, and hence there is the possibility of cross-saturation between phases, reducing the torque. This is most likely to occur

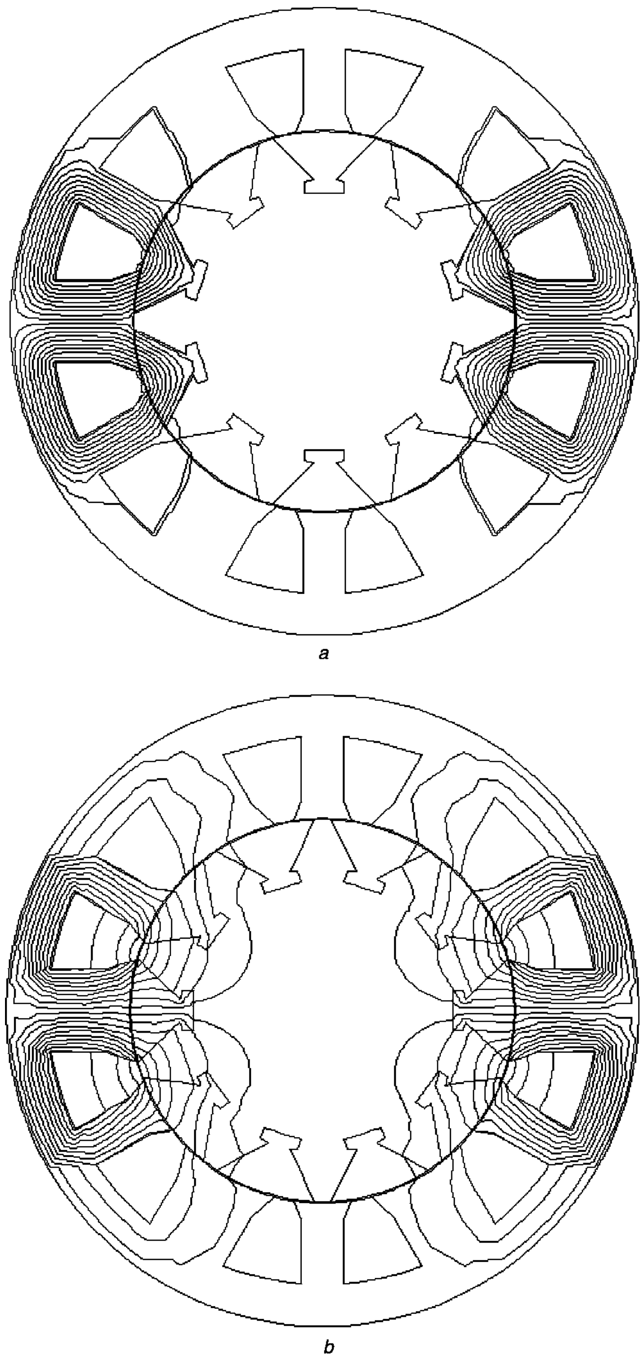

Fig. 8 *Magnetic flux plots for 12–10 single-tooth winding machine with a single-phase excited in aligned and unaligned positions*
a Aligned position
b Unaligned position

when the machine is operating under voltage control and positive voltage is applied for more than one-third of a cycle. Under all other operating conditions the cross-saturation effect will be negligible.

The above effect can be removed completely if the MMFs of adjacent stator coils are directed in the opposite direction, i.e. inwards, outwards, inwards, outwards etc. When this occurs the unwound teeth carry the difference between the flux of adjacent coils, and hence simultaneous excitation of two phases will actually reduce the saturation conditions in this region. Note that with this arrangement the unwound teeth carry bi-directional flux.

In addition to having a minor influence on the torque capability of the machine, the direction of the stator coil MMFs influences the iron loss in the machine, but this is beyond the scope of this paper.

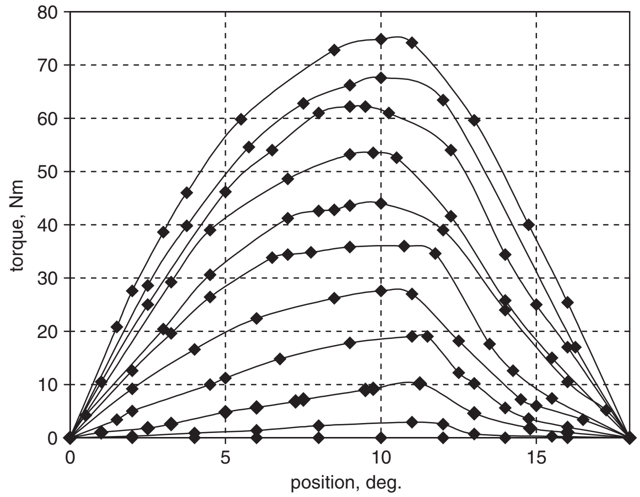

Fig. 9 *Measured static torque curves for 12–10 single-tooth prototype with a single-phase excited*
Each curve is for a constant current, rising in 2.0 A steps to 20.0 A

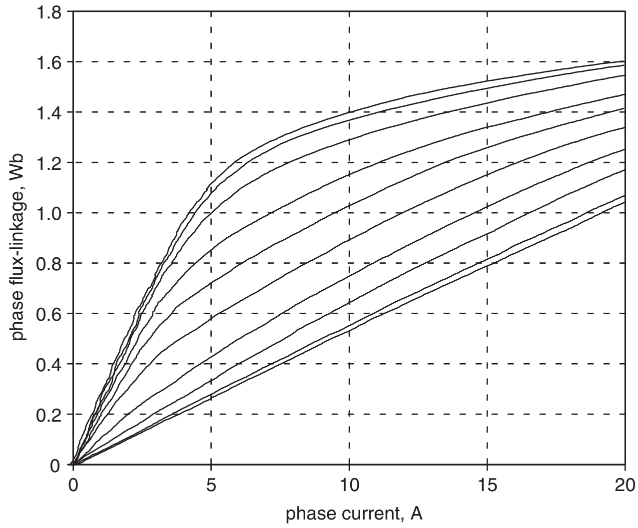

Fig. 10 *Measured flux-linkage curves for 12–10 single-tooth prototype with a single-phase excited*
Each curve is at constant position, running from unaligned to aligned positions in 2.0 deg. steps

7 Running tests

The machine has been coupled to a three-phase asymmetric half-bridge inverter and subjected to an extensive series of running tests. The inverter employed IGBTs, fed from a 590 V DC link, switching at 20 kHz, with rotor position measured using a 12-bit optical encoder. The rotor position and phase currents were fed back into a DSP based PI controller, which implemented the phase current control. The current demand for each phase was constant during its desired conduction period and zero for the rest of a cycle. The machine was coupled to a DC load machine, via a torque transducer, capable of measuring up to 100 Nm.

For all running tests the measured currents and torque output corresponded closely with those values predicted using the static flux-linkage and torque measurements. This indicates that the static and dynamic parameters are virtually identical and there are no major unforeseen effects occurring within the machine. Example results for the drive are given below.

Fig. 13 shows measured voltage and current waveforms with the machine operating at a speed of 536 rev/min and a current demand of approximately 10 A. Positive voltage is

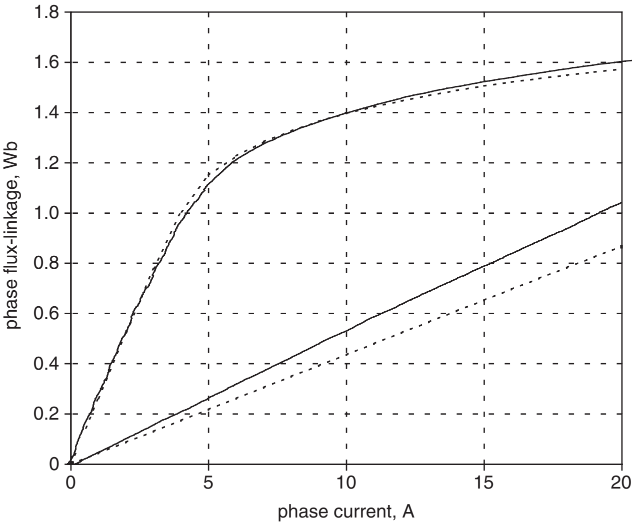

Fig. 11 *Comparison between measured flux-linkage and those predicted using 2D finite elements*
Both unaligned and aligned positions are shown
—— measured; ------ predicted

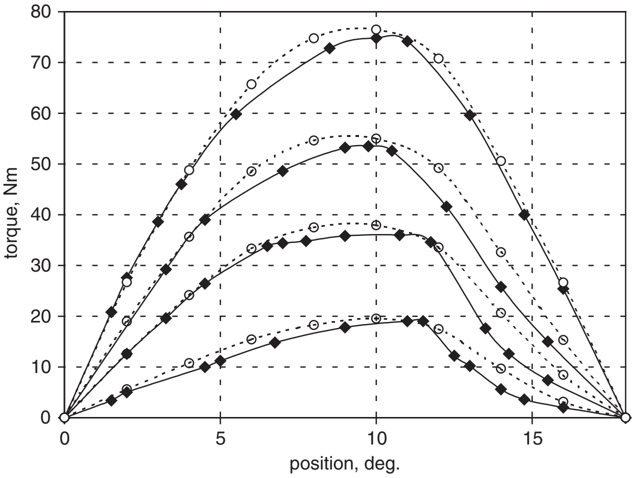

Fig. 12 *Comparison between measured static torque curves and those predicted using 2D finite elements*
Curves shown are for 5, 10, 15 and 20 A of excitation
—— measured; ------ predicted

first applied to each phase 9 electrical degrees after the unaligned position, with the current demand remaining high for an angle of 123 electrical degrees. As can be seen in Fig. 13, the machine operates under current control, with each phase conducting for one-third of a cycle. The mean torque was evaluated from the output of the shaft mounted torque transducer and was measured to be 29.0 Nm. From integration of the applied voltage using (1) the flux-linkage has also been determined and hence the flux-linkage/current locus plotted. This locus is typical of a switched reluctance motor operating with a degree of current control. The torque transducer is bandwidth limited so that it measures a relatively small torque ripple at this speed, but it is likely that the electromagnetic torque has relatively large pulsations. From knowledge of the static torque characteristics a peak–peak electromagnetic torque ripple of up to 30% of the mean torque is predicted.

Fig. 14 illustrates full voltage control at a speed of 1100 rev/min. The phase switch on angle has been advanced to 18 electrical degrees before the unaligned position, with a phase conduction angle of 158 electrical degrees. Hence negative voltage is applied to the phase winding 40 electrical

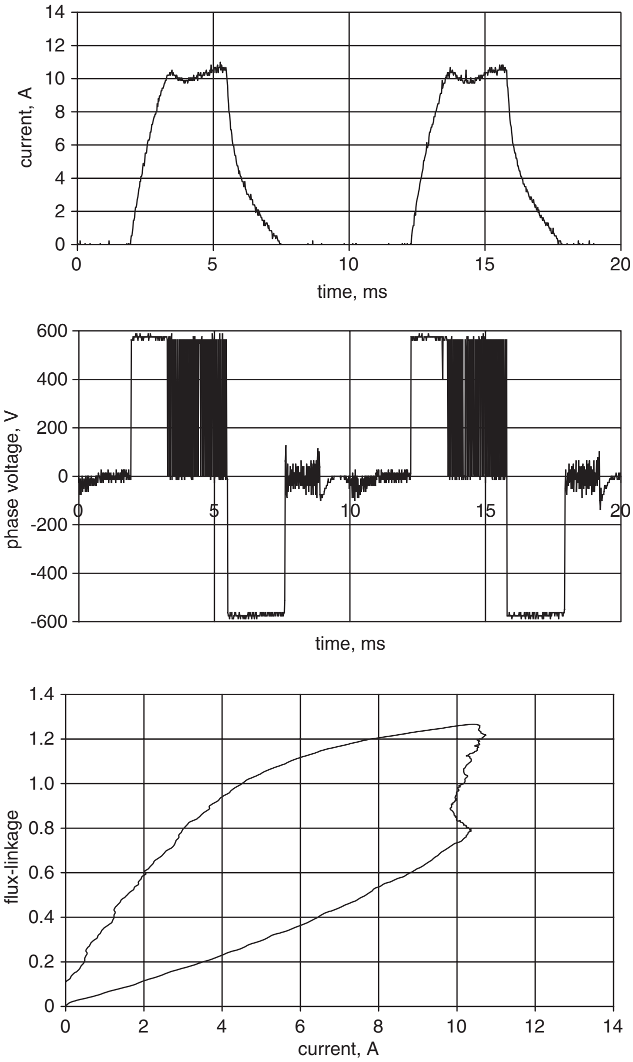

Fig. 13 *Measured phase current, voltage and flux-linkage locus for drive operating under current control at a speed of 586 rev/min*
Phase switch on angle 0.9 deg. after unaligned position, conduction angle 12.3 deg. Measured mean shaft torque = 29.9 Nm

degrees before the aligned position is reached. By applying full voltage early in the cycle the current builds up quickly and the flux-linkage/current locus continues to enclose a large area, resulting in a mean measured torque of 25.2 Nm.

The machine has been thermally tested during operation, with temperatures monitored using thermocouples on the frame, laminations and embedded within the winding. The machine exhibited two thermal time constants: one of 45 min associated with bulk heating of the entire machine and frame and accounting for 56% of the steady-state temperature rise, and one of 3 min associated with heating of the winding and accounting for 44% of the temperature rise. Operation at 500 rev/min could sustain 32 Nm for a steady-state temperature rise of 100 °C.

8 Comparison with other switched reluctance machines

The single-tooth winding prototype machine has been found to have a very low thermal impedance between the winding and frame and therefore performs very well thermally. In the authors' experience single-tooth windings generally have good thermal performance; however, this feature is very dependant on the slot liner type and the degree to which the winding is impregnated with resin, rather than the electromagnetic design. An objective

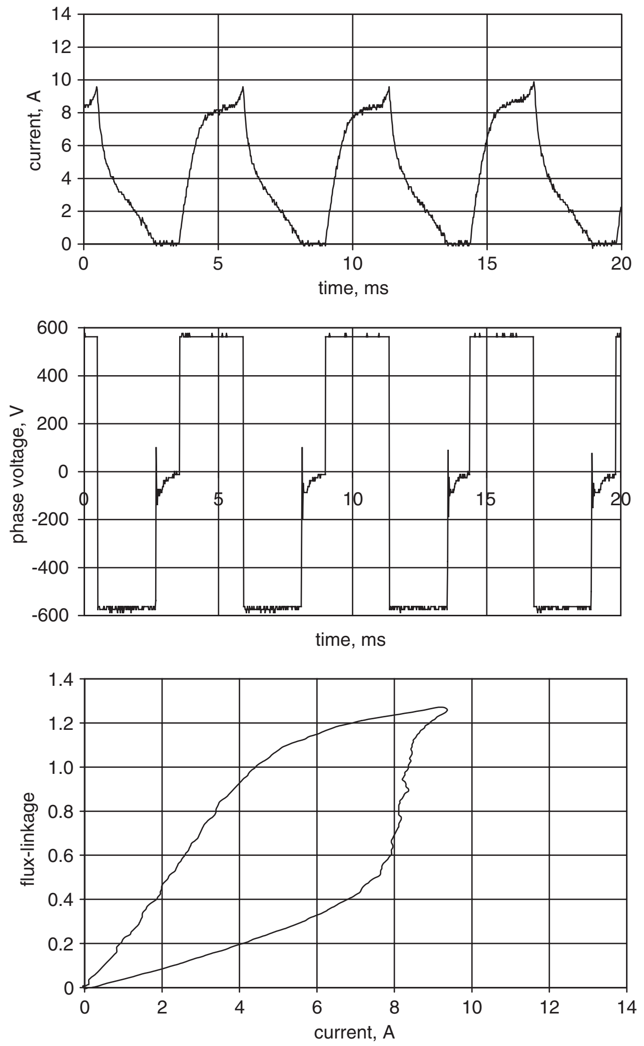

Fig. 14 *Measured phase current, voltage and flux-linkage locus for drive operating under voltage control at a speed of 1100 rev/min*
Phase switch on angle 1.8 deg. before unaligned position, conduction angle 15.8 deg. Measured mean shaft torque = 25.2 Nm

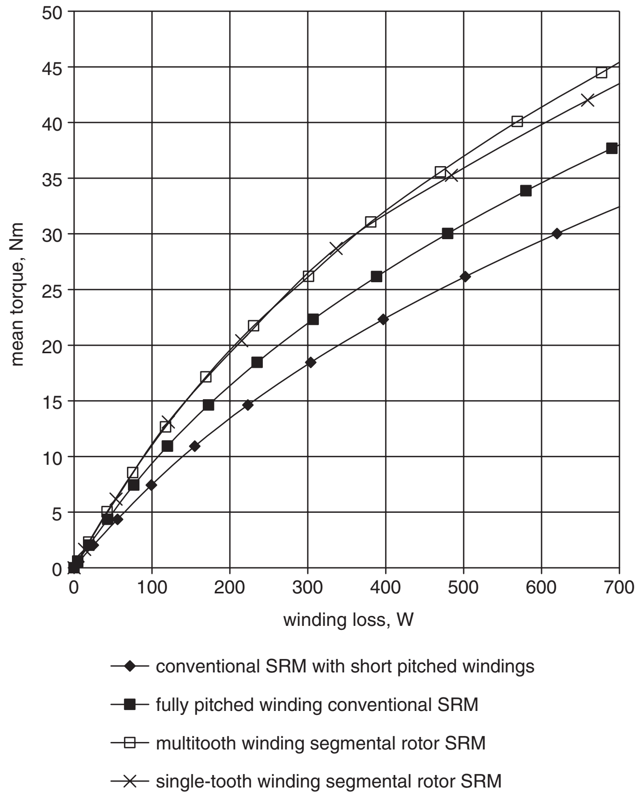

Fig. 15 *Mean torque production as a function of winding loss for conventional and segmental SRMs, assuming perfect current control with each phase conducting for one third of a cycle*
Winding temperature = 100 °C

comparison with other machines is most easily made on the basis of loss, rather than temperature rise, as there is no longer the necessity to have equality of cooling systems and winding techniques.

Fig. 15 shows the mean torque produced as a function of winding loss for the prototype machine, alongside those for the multitooth winding segmental SRM and two conventional SRMs, one with short pitched windings and one with fully pitched windings. All four machines have the same outside diameter and lamination stack length and all results are based on measured static torque performances. For the purposes of this comparison it is assumed that each machine is operating under current control with one phase conducting at a time. Throughout the phase conduction period the phase is assumed to conduct a constant current and the torque output is based on the mean measured torque over the period of conduction. Losses presented are based solely on winding losses, using the winding resistance of each machine when running at an average winding temperature of 100 °C.

At all loss levels the segmental machines produce substantially more torque than the conventional SRMs. For 300 W of winding loss, which is comfortably within the thermal limit of all four machines, the conventional SRM produces 18.4 Nm, the fully pitched winding conventional SRM 22.0 Nm, the multitooth winding segmental SRM 26.1 Nm and the new single-tooth winding segmental SRM 26.5 Nm. Hence, in broad terms the single-tooth winding segmental machine is producing the same torque as the multitooth winding segmental machine. Whilst it has the same core volume as the earlier segmental design, it is achieving the same performance with only 71% of the copper volume.

9 Conclusions

A design of switched reluctance motor, combining a segmental rotor with short pitched windings, has been designed, built and extensively tested. The concept enables a large increase in the flux linking each turn of the machine, thereby creating a large increase in torque density. The machine delivers 44% more torque than a conventional SRM and equals the torque capability of an earlier segmental SRM design [1, 2] with windings spanning three teeth, whilst using 29% less copper volume. In comparison to the earlier segmental design the windings are used more efficiently because of the shorter end-winding length, but the magnetic performance is reduced: these two effects approximately balance out to give equal torque capability.

Measured flux-linkage and torque characteristics are in line with those predicted using the finite element method. During operation as a drive, supplied with current from three asymmetric half-bridges the machine continues to perform in line with predictions. Static torque at thermal limit is over 30 Nm in a machine of 150 mm outside diameter and 150 mm lamination stack length.

The design offers an advantage over segmental rotor SRMs, with windings spanning multiple teeth, due to the short length of the end-windings. This makes the concept particularly suitable for machines of a relatively short axial length and removes the limitation of the earlier multitooth segmental designs.

The concept has many of the attributes desired for a fault tolerant drive: the windings are magnetically, thermally and mechanically isolated from each other to a greater degree than in a conventional SRM. The machine may therefore be particularly suitable for such applications. However, the high torque density achieved suggests that its applications may be more widespread. Further research is required to determine other performance issues, such as iron loss and acoustic performance, as well as issues related to mass production of such a machine.

10 Acknowledgments

The authors would like to thank the UK Engineering and Physical Sciences Research Council for funding this work and Switched Reluctance Drives Ltd. for their industrial collaboration. They would also like to thank Mr. P.G. Dickinson for his advice regarding the mechanical construction and Mr. C. Manning for building the prototype machines.

11 References

1 Mecrow, B.C., Finch, J.W., El-Kharashi, E.A., and Jack, A.G.: 'Switched reluctance motors with segmental rotors', *IEE Proc., Electr. Power Appl.*, 2002, **149**, (4), pp. 245–254
2 Mecrow, B.C., Finch, J.W., El-Kharashi, E.A., and Jack, A.G.: 'The design of switched reluctance motors with segmental rotors'. 15th Int. Conf. on Electrical machines, Brugge, Belgium, August 2002
3 Mecrow, B.C.: 'Switched reluctance electrical machine', UK Patent Application No. 0209794.7, 30 April 2002
4 Lawrenson, P.J., and Agu, L.A.: 'Theory and performance of polyphase reluctance machine', *Proc. Inst. Electr. Eng.*, 1964, **111**, (8), pp. 1435–1445
5 Lawrenson, P.J., and Gupta, S.K.: 'Developments in the performance and theory of segmental-rotor reluctance machines', *Proc. Inst. Electr. Eng.*, 1967, **114**, (5), pp. 645–653
6 Longya, X., Lipo, T.A., and Rao, S.C.: 'Analysis of a new variable-speed singly salient reluctance motor utilizing only two transistor switches', *IEEE Trans. Ind. Appl.* 1990, **26**, (2), pp. 229–236
7 Longya, X.: 'Design and evaluation of a converter optimised synchronous reluctance motor drive'. PhD Thesis, University of Wisconsin-Madison, 1990
8 Lipo, T.A., and Longya, X.: 'Variable speed machine with high power density', United States Patent No. 5,010,267, 23 April 1991
9 Horst, G.A.: 'Isolated segmental switched reluctance motor', United States Patent No. 5,111,096, 5 May 1992